CONF/781009-1
UC-90, 93

IV U.S.-U.S.S.R. Colloquium
on MHD

Results of Tests and Studies of American Materials in the Channel of the MHD Facility U-02 (Phase III)

LATE PAPER

D. K. Burenkov, T. I. Borodina, D. A. Vysotsky,
V. I. Zalkind, V. V. Kirillov, A. I. Romanov,
G. P. Telegin, N. V. Strekalov

In accordance with the U.S.-U.S.S.R. Cooperative Program in MHD joint U.S.-U.S.S.R. tests were conducted in May 1978 at the U-02 facility of an MHD generator section consisting of U.S.-built electrode blocks and U.S.S.R.-built insulating walls. The main purpose of the experiment was to conduct continuous 100-hour duration tests of materials and structures of electrode blocks; in particular, to study the behavior of ceramic electrodes and insulators in operating conditions of an MHD generator, the electro-physical and thermal characteristics of the working section as a whole and electrodes in particular, and to analyze the change in the phase composition and structure of materials during the test.

The main thrust of the experiment was a study of electrode material behavior. If during the U-02 test, phase I and II, attention was primarily directed at evaluating the behavior of electrodes based on stabilized zirconium dioxide, then the last, phase III experiment involved the testing of electrodes with lanthanum chromite base.

Chromites are a very interesting class of oxide compounds with a high melting point (from 2500°C for $LaCrO_3$ to 2200°C for chromites at the end of the lanthanoid series). The ordinary chromites at normal temperature have a relatively high specific electrical resistivity (10^3 ohm/cm). However, heterovalent doping of chromites with alkaline earth oxides (CaO, MgO, SrO) can radically decrease the value of electrical resistivity (10-50 ohm/cm). Unlike stabilized zirconium dioxide, doped chromites have a high conductivity

in the low temperature range (figure 1), electronic conductivity mechanism and highter thermo-conductivity - all these are of significant importance when the doped chromites are used for MHD generator electrodes.

Six varieties of electrodes based on doped lanthanum chromite were tested and investigated. The compositions of these six groups of electrodes are shown in Table 1. The electrodes were made of fine grained, hot-pressed mass (the porosity of the ceramic was 2-3%). The interelectrode insulators were made of magnesial and magnesial-spinel ceramic also manufactured by the hot pressing method (Table 1).

In order to increase the thermal stability of the ceramic, the fine segmentation principle was employed. The electrode walls consisted of 36 pairs of electrodes. Each electrode element consisted of water cooled copper base with three or four ceramic elements soldered to it (figure 2). In order to diminish the thermal stresses the attachment of ceramic to the copper base was accomplished through an intermediate layer of nickel mesh (figure 3). Each copper base with electrodes and insulators located between them was mounted on the common base-plate made of fiberglass (figure 4). Figure 5 shows the electrode block prior to the test (figure 5). The insulating walls of the channel were made of ceramic modular walls, as they were during phase I and phase II. The magnesial ceramic for these walls was manufactured from a grainy mass by conventional pressing and subsequent baking (porosity 12-14%). The U-02 facility and its main operating parameters have been discussed in detail in reports of phase I and phase II of the tests.

The joint experiments at the U-02 were conducted in accordance with the previously agreed working program and included the following basic stages:

1) preliminary hydraulic and electric tests of the channels,

2) preheating of the loop and selection of thermal conditions for duration tests,

3) measurement of electrophysical characteristics of the experimental section and determination of the electrical loading parameters for duration tests,

4) duration tests,

5) cooling of the loop,

6) post-run tests and disassembly of the experimental section.

The preliminary tests showed that hydraulic and electrical characteristics of the section were in accordance with the technical requirements. In particular, the average level of electrical insulation between individual elements of a section was, on the average, 100 kohm when tested with a voltage up to 1 kV.

The preheating of the loop was initially carried out by turning on the air preheater that heats the air to 250°C. Then the combustion chamber was started up at α = 2.5, gradually increasing the combustion product temperature and preheating the elements of the structure at the rate of 1.5-2°C/min.

The basic operating mode for the loop at the parameters is listed in Table 2. These parameters were maintained during the duration test stage of the experiment.

Considerable attention during this test was directed at determining the temperature condition of the section elements and first of all temperatures on the surface of the electrodes. For this purpose thermocouples were installed in the electrodes at varying depths from the hot surface and thermal fluxes passing through each electrode group were measured. In addition, an optical pyrometer was used to measure the temperature of the surface on the first electrode of the second group on the anode wall (2207).

The temperature of the electrode surface measured by means of an optical pyrometer was 1570-1620°C. Taking into account the fact that the pyrometer was not focused on the center electrode, the actual temperature of the hottest portion of the electrode was 1700°C which is in good agreement with the preliminary thermal calculations.

The analysis of the data from the thermocouples located in the electrode blocks, and particularly thermocouples located near the surface, showed that the measured temperatures were on the average close to the calculated. The difference between the thermocouple readings and the calculated values was within $\pm$ 100°C range. It has to be kept in mind that the preliminary analysis of the thermocouple reading error with due regard for the errors in installation, instrumental error and difference in thermal conductivity of thermocouple material and electrode material, etc., was in the range of $\pm$ 100-110°C.

Thus, the maximum electrode block surface temperature on the anode wall should be characterized as follows:

1st group	1650-1750°C
2nd group	1600-1700°C
3rd group	1600-1700°C
4th group	1550-1650°C
5th group	1500-1600°C
6th group	1500-1600°C

The temperature on the cathode wall because of a slight slanting of the flow was 50-70°C lower than the corresponding values on the anode wall.

The thermal operating mode analysis for the insulating wall showed that the surface temperature of MgO insulating modules is 1500°C.

Characteristic changes in the thermal fluxes during the experiment is shown in figure 6, where thermal fluxes of the 6th group of electrodes

(anode wall) are cited as the example. The curve shows that fluctuations of the thermal flow during the experiment are on the average about 10%. By the end of the duration tests there was an insignificant reduction in the thermal flux. This tendency is characteristic for all the groups of electrodes with the exception of the third cathode block where the thermal flux was reduced by approximately 20% compared with the initial value. The average thermal flow on the anode wall is approximately 1.2 times higher than the thermal flux on the cathode wall. A comparison with the data of preliminary thermal calculations shows that the experimental thermal flux in the center of the section is on the average 10% lower than the calculated value while at the extreme sections the difference may be as great as 30%; this can be explained by the radiation to the sections that are more intensively cooled, located both upstream and downstream of the experimental section.

The third stage of the test included the study of electro-physical characteristics of the electrodes and the working section at constant flow parameters selected for the duration tests.

The resistance of insulation between channel elements was subjected to a series of tests. Measurements showed that the insulation resistance between adjacent cathodes and anodes before the beginning of duration tests was, as a rule, 60-150 ohm. The effective resistance of the anode-cathode insulation calculated in accordance with the channel characteristics in induction mode was approximately 500 ohm. This shows good agreement with the measured values of insulation between elements. The effective resistance of insulation anode-cathode is approximately by an order of magnitude higher than the effective resistance of plasma. The measured resistance of channel insulation in the axial direction is also more than 5 times greater than the

experimentally determined resistance value of the plasma along the channel which consists of a value of about 5 ohm and is close to the calculated value.

Prior to the duration tests preliminary studies of the electrical characteristics of electrodes and the channel as a whole were conducted in the generating mode, in particular, in open circuit mode and short circuit mode. The open circuit mode voltage was 150-160 V, the short circuit currents were 2.0-4.0 A (see Table 3). The average figure for the channel as a whole was 2.9 A/electrode which corresponds to the average current density of approximately 0.45 A/cm^2. The maximum short circuit currents (about 3.4 A) were observed in the electrodes of group 5 (70% $LaCrO_3$ + 30% ZrO_2 with platinum current leadouts on the cathodes) the smallest currents (see Table 3) were observed on the electrodes of the 1st and 4th groups (2.7 and 2.27 A). These groups consisted respectively of 70% $LaCrO_3$ + 30% ZrO_2 and of lanthanum chromite doped with magnesium. Relatively small currents on the last group of electrodes were evidently connected with a lower temperature on their surface compared with the preceeding groups. The reduction of currents in the first group of electrodes as well as in the reduction of thermal fluxes to its surface was also possibly contributed to by the relatively low temperatures of the nozzle section of the loop upstream of the working section of the channel.

Distribution of electrode potentials in the short circuit mode of all electrode pairs was uniform along all of the channel and Hall voltage was 170-180 V, which was 25-30% lower than the maximum possible value for the induced Hall voltage.

Thus, analysis of the electrical characteristics of the channel shows that the resistance level of the insulation in the insulating walls of electrode

modules before the beginning of duration tests was quite satisfactory and has little effect on the characteristics of the channel and individual pairs. The electrical characteristics of the channel were in satisfactory agreement with the estimates that took into account certain actual effects, such as non-uniformity of plasma conductivity in the presence of boundary layers, Hall effect and the finite resistance of the insulation.

The overall operating time for the channel section at constant thermal parameters was 107 hours, including 100 hours of duration tests.

During the duration tests of electrodes under current, as well as during the first and second phase of joint experiments at the U-02, each group of electrodes was expected to operate at two values of current density: approximately 1.25 A/cm^2 and in the range between 0.4-0.6 A/cm^2. As in the preceeding experiments current density about 1.25 A/cm^2 was ensured on individual electrode pairs by means of connecting to them separate current sources decoupled from the potential (all together 10 sources), so that these pairs operated in "stagnation mode" (even though it was close to short circuit mode). The currents 0.4-0.6 A/cm^2 were supplied to the electrode pairs in the short circuit mode. In addition, in each group of electrodes there were 1-2 pairs that operated in the disconnected circuit mode, i.e., without current, serving as "reference samples".

During the duration tests measurements of thermal fluxes to the channel elements, readings of thermocouples, distribution of currents and voltage to electrode pairs, as well as the distribution of potential of electrodes and probes, were performed every hour. The preliminary data on operation of electrodes during the duration tests were shown in Table 4.

The current on the electrode pairs loaded from external sources was maintained constant within the limit between 7.0 to 8.0 A (1.25 A/cm^2). The

voltage of the sources varied between 30-120 V at the beginning of the test to 20-50 V at the end. The voltage increased primarily along the channel. The absolute majority of loaded electrodes (9 out of 11 pairs) has survived the entire cycle of duration tests (100 hours).

During the tests the current of electrode pairs connected in short circuit mode, gradually decreased (from 4-5 to 1-2 A and more). This was particularly conspicuous on the pairs adjacent to those loaded from external sources: currents on these pairs gradually decreased, on some pairs to zero or even to a reversed sign. In view of this unstable operation of the electrodes (approximately up to 70-75 hours of the duration tests) 12 pairs of electrodes were transferred from short circuit mode to open circuit mode.

During the duration tests there were also changes in the distribution in the potentials of electrodes along the channel. The groups of adjacent electrodes acquired similar potentials while the main Hall voltage drop along the channel was, as a rule, noted near the interface between groups. The overall Hall voltage under those circumstances was somewhat reduced (180-160 V).

The analysis of the distribution of potentials and currents to the electrode pairs during duration tests showed that the cause of these changes in the characteristics was a gradual reduction of insulation between adjacent electrodes. The reduction in insulation was determined by direct measurements made following the shut-down of seed injection in the middle of phase 3 duration tests. Thus, resistance between adjacent electrodes and the anode wall was from 1-3 to 20-40 ohm.

In addition to the intial program of the duration tests, studies of channel characteristics in open mode operation and short circuit mode opera-

tion of all pairs were conducted every 12 hours. These measurements showed that the electrical characteristics of the channel differed little in time (see Table 3): the average short circuit current to one pair 2.9-2.7 A, the open circuit voltage from 150-160 V to 50-170 V, the Hall voltage between 170-190 V to 156-170 V, although the potential distribution to the electrodes along the channel by the end of the tests was not uniform.

Following the completion of duration tests, volt-ampere characteristics of the channel were studied in induced field and insulation was measured. The open circuit voltage was 150-170 V, the level of insulation between anodes was within the range between 1 ohm (in the second portion of the channel) and 40 ohm. It should be noted that during the electrical duration tests of the electrodes, the nickel current leadouts demonstrated high performance capability. There was not one single case of electrode failure because of current leadout breakdown. Visual inspection of cathode and anode walls after the tests showed them to be in satisfactory condition (figure 7).

Thus, there was a perceptible difference in the degree of erosion in each electrode group (Table 5). In the order of increased erosion, electrode groups may be placed in the following order: 4, 5, 2, 3, 6, 1. If the depth of the erosion on electrodes of groups 4 and 5 was on the average 1-3 mm, for individual electrodes in groups 2 and 6 it attained the depth of 7-10 mm. The greatest erosion was noted in the central section of the electrode walls. Sections adjacent to the insulation panels were the least damaged.

After the tests the electrodes had either a porous, uneven surface, or a black, smooth surface with white inclusions (figure 8). In some cases adjacent electrodes on the anode wall were connected by a deposit of porous texture or by a brown film.

It does not appear to be possible to establish the difference in the erosion durability of electrodes operating with current and without current. Electrodes operating without current (1101, 1207, 2313) showed greater damage than the electrodes working with current (1105, 2318).

Thermal cracks were observed only in electrodes of the 4th group.

The interelectrode insulators showed greater thermal and erosion damage than the electrodes (Table 5), while the insulators made of spinel were more durable than insulators made of magnesium ceramic.

The state of insulating walls after the test was quite satisfactory. The insulating walls showed the same high performance capability as during phase I and 2 of the U-02 tests.

The tested electrode insulation materials were investigated using the X-ray spectral, X-ray structural and microscopic analysis methods. A coherent pattern of phase and structural changes occuring in the materials during the experiment and during the subsequent storage was established.

The studies demonstrated that of the two main phases present in the tested electrodes (doped lanthanum chromite and stabilized zirconium dioxide) the greatest changes occured in the doped lanthanum chromite. In the hot zones of the electrodes a decrease in the volume of the unit cells of the orthorhombic perovskite has been noted as well as the redistribution of Mg and Al in the crystalline lattice of the orthorhombic perovskite, the appearance of phases enriched with Al and depleted of Mg, the isolation of dependent phase of magnesium chromite, partial decomposition of lanthanum chromite and formation of chromium and lanthanum oxides, hydration of lanthanum oxide with formation of lanthanum hydroxide. The smallest changes in chromites were noted in electrodes of the second group. Precisely these electrodes in their initial state contained a minimum amount of admixtures. The initial electrodes of other groups, especially 1 and 6, contained in their composition admixtures of $La(OH)_3$,

La_2CO_5, $MgCrO_4$, $La_2Zr_2O_7$. Evidently, the presence of these admixtures indicates a diminished stability of chromites in these materials.

On the working surface of the tested electrodes (for all groups) as well as at the depth of 2-3 mm from the surface (for groups 1, 2, and 3) lanthanum zirconite is present, $La_2Zr_2O_7$. Its presence indicates that an interaction reaction between the products of partial decomposition of lanthanum chromite (La_2O_3) with zirconium dioxide, present in the material or deposited on its surface as a result of carry-over from the combustion chamber, occurs. In the materials of all the electrodes the formation of such phases as $MgCrO_4$ and $MgCr_2O_4$ is noted. The appearance of these substances is dependent both on the processes of magnesium redistribution in the lanthanum chromite lattice and on the reaction of electrode materials with insulation material.

It has been established that on the interface between electrode and insulator there occurs an intensive mutual diffusion of phases included in the electrode and insulation materials. As a result, in the hot zones of the insulators $MgCr_2O_4$, $MgCrO_4$, $LaCrO_3$, $La_2Zr_2O_7$, Cr_2O_3, $La(OH)_3$ are recorded. In the cut of the tested electrodes the formation of a light-brown layer is observed near the hot surface and of bright green zones in the central portion (especially on the cathodes).

The amount of potassium compounds (K_2CO_3, $KHCO_3$, KOH) that have penetrated into the tested electrodes and have a high degree of density is relatively small. The potassium compounds are located primarily in the zones that have sustained the greatest changes compared with the initial material. Here a product of lanthanum chromite with alkaline seed has been found, but so far has not been fully identified. It should also be noted that the instrusion of seed is more conspicuous on the cathode than on the anode. The process

leading to the change in the phase composition and in the structure of the initial material in the cathode is also more pronounced than on the anode.

Thus, duration tests and post-test analysis made it possible to obtain useful information concerning the behavior of electrode and insulator materials and structures in the conditions of duration operation. The results of these experiments made it possible to attain greater understanding of the processes occuring in the electrodes with lanthanum chromite base.

During the U.S.-U.S.S.R. duration tests at the U-02 facility (phase 1-3, 1975-1978) an improved methodology for conducting the experiments has been perfected, the structure of electrode walls and current leadouts was improved. A broad range of electrode and insulation material was tested and this made it possible to select the most promising technical solutions for development of materials and structures of the future MHD generator channels.

Table 1

Electrode Compositions

Group #	Electrode #	Composition	Current Leadouts	Insulator
I	I-6 (cathode) I-7 (anode)	70 mol.% $La_2Cr_2O_3$ (5% MgO) 30 mol.% ZrO_2 (9% Y_2O_3)	pressed nickel mesh (5.0 mm)	MgO
2	7-II (cathode) 8-II (anode)	$La_2Cr_{1-x}Al_xO_3$ (2% MgO) layered (2 layers of equal thickness)	-"- (5,0 mm)	MgO
3	I2-I8	70 mol.% $La_2Cr_2O_3$ (5% MgO) 30 mol.% ZrO_2 (9% Y_2O_3) layered	-"- (2,5 mm)	MgO
4	I9-24	$La_2Cr_2O_3$ (5% MgO)	-"- (2,5 mm)	$MgAl_2O_4$
5	25-30	70 mol.% $La_2Cr_2O_3$ (5% MgO) 30 mol.% ZrO_2 (9% Y_2O_3)	-"- (5,0 mm) 1 mm platinum (only on the cathode)	$MgAl_2O_4$
6	3I-36	$La_2Cr_2O_3$ (2% MgO)	pressed nickel mesh (2,5 mm)	$MgAl_2O_4$

Table 2

Basic Operating Parameters of U-02

Plasma temperature at the entrance to the channel, K	2570-2600
Pressure in the combustion chamber, Ata.	0,93-0,95
Mass flow rate, kg/sec	0,73-0,75
Ionizing seed concentration (K), Wt. %	I
Degree of oxygen enrichment, Wt. %	50-52
Plasma conductivity, mho/m	5-7
Coefficient of of oxidizer (α)	I

Table 3

Average Currents to the Electrode Pairs in Short Circuit Mode of the Generator in the Range of Open Circuit Voltage in Each Group of Electrodes at Different Times During Tests

Group #	I		II		III		IV		V		VI		V_{Hall}
Electrodes	a	B	a	B	a	B	a	B	a	B	a	B	voltage
Time	I_{K3}	V_{xx}	I_{K-3}	V_{xx}	I_{K3}	V_{xx}	I_{K-3}	V_{xx}	I_{K3}	V_{xx}	I_{K-3}	V_{xx} [xx)]	
I4.05.78 II.40-II.25	2,70	II0-I40	2,84	I45-I55	2,89	I55-I58	2,98	I55-I57	3,35	I50-I57	2,57	I25-I50	I73
I5.05.78 II.00-II.I5	2,53	82-I35	2,69	I38-I48	2,57	I40-I5I	2,84	I47-I50	3,24	I39-I47	2,8I	I25-I5I	I80
I7.05.78 00.30	2,63	72-I24	2,84	I53-I6I V_{K8} = I36 V	2,66	I65-I67 V_{K4} = I3I V	2,62	I67-I68	3,55	I55-I65	2,87	I03-I52	I70
I9.05.78 00.10	2,3	[x)]95-I26	3,04	I59-I68 V_{K8} = I38 V	I,72	I69-I73	2	I68-I73	4,2	I62-I70	3,7	97-I63	I8.05.78 V_x = I50 V I64

[x)] $V_{xx\,(1-2)}$ = 3I÷55 V

[xx)] without 36 pairs V_{xx} = 75÷II0 V

Table 4

Working Conditions of Electrodes during Duration Tests

Pair #	XX, time, hr	K3		Loading		Pair #	XX, time, hr	K3		Loading	
		time, hr	current, A	time, hr	avg. A current			time, hr	current, A	time, hr	avg. A current
I	I00					I9				I00	-7,94
2	26	74	2,6-6			20				I00	-7,36
3	26	74	0,3-I,8			2I	28	72	0,5-0,8		
4				I00	7,I6	22	26	74	0,4-3,7		
5				I00	7,52	23		I00	I,2-4,2		
6	30	70	I5-3,8 55,0- 0,2+0,5			24	I00				
7	I00					25	I00				
8		I00	2,3-4,6			26		I00	0,3-5,7		
9		I00	2,4-3,9			27	30	70	0,7-3,6		
I0		I00	0,7-4,6			28	28	72	0,7-I,9		
II		I00	0,9-3,5			29				I00	7,67
I2	I00					30				I00	7,40
I3	I00					3I				I00	7,03
I4	I00					32				I00	7,45
I5	27			73	7,52	33	50	50	I-3		
I6	30	70	0,3-I			34	30	70	0,6-3,4		
I7	74			26	7,38	35	28	72	I,6-4,8		
I8				I00	-7,08	36	I00				

Table 5

Degree of Erosion of Electrodes and Insulators
Based on Visual Inspection of Walls (mm)

Electrode Group #	Composition of Electrodes & Insulators	Cathode		Anode	
		Electrode	Insulator	Electrode	Insulator
I	70% $LaCrO_3$ + 30% ZrO_2 MgO	5-7*)	[redacted] 7-10	5-7*)	[redacted] 8-10
II	$LaCrO_3$ - $LaAlO_3$ MgO	5-7*)	[redacted] 7-10	I-2	10-12
III	70% $LaCrO_3$ + 30% ZrO_2 MgO	I-3	5-7	7-10*)	10-13
IV	$LaMgCrO_3$ $MgAl_2O_4$	0-I	0-I	I-2*)	I-2
V	70% $LaCrO_3$ + 30% ZrO_2 $MgAl_2O_4$	I-3	2-5	I-2	0-I
VI	$LaMgCrO_3$ $MgAl_2O_4$	I-10*)	10-13	0-I	I-5

*) Degree of erosion on the central portion of the electrode wall.

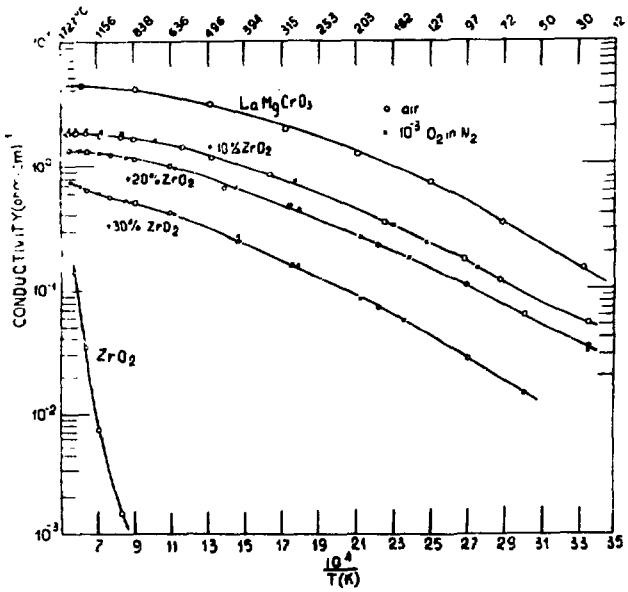

Figure 1. Temperature dependence of electrical conductivity of doped lanthanum chromite and stabilized zirconium dioxide.

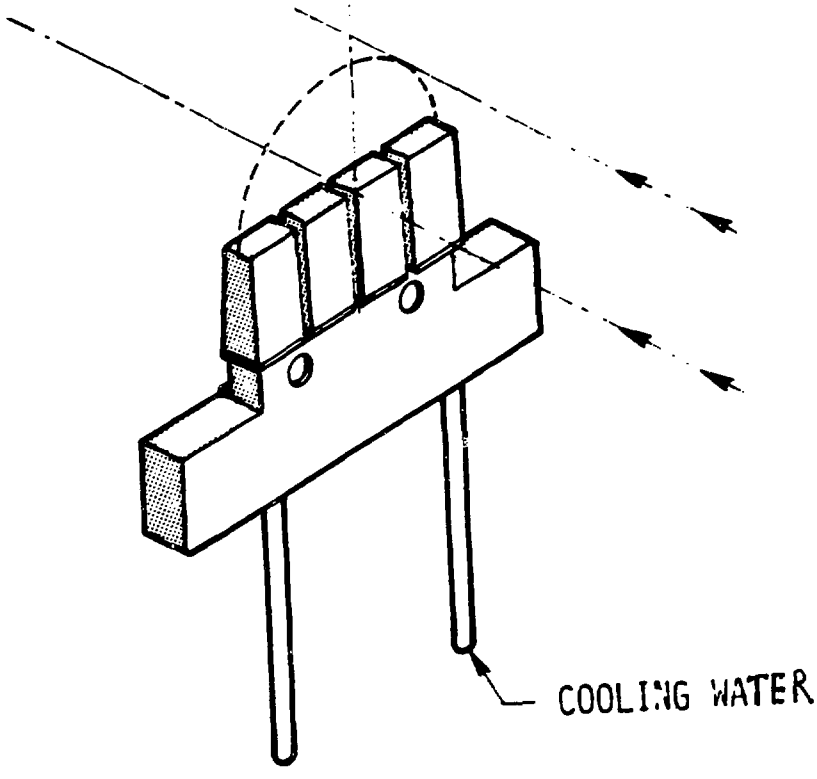

Figure 2. Diagram of individual element (copper base with ceramic electrodes) of the electrode wall.

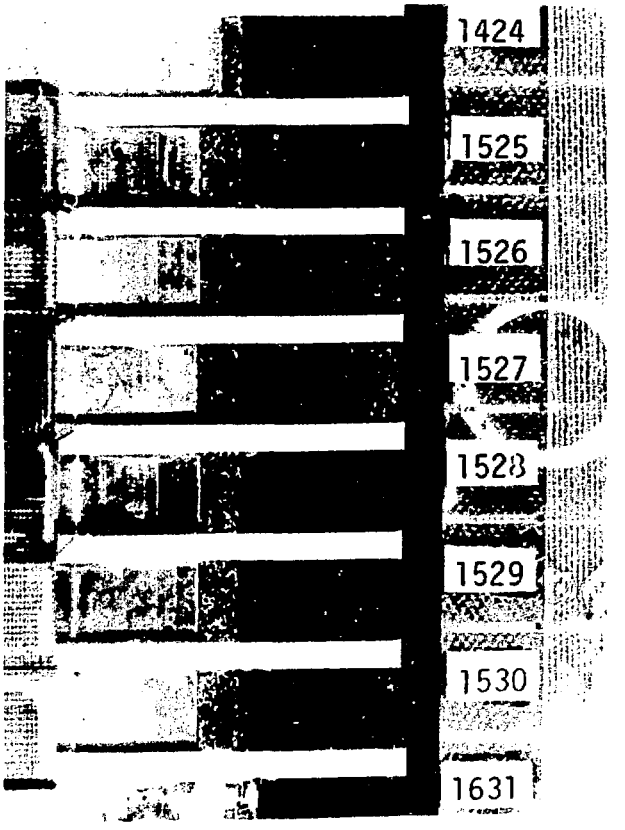

Figure 3. Interface between the chromite electrodes and the copper base.

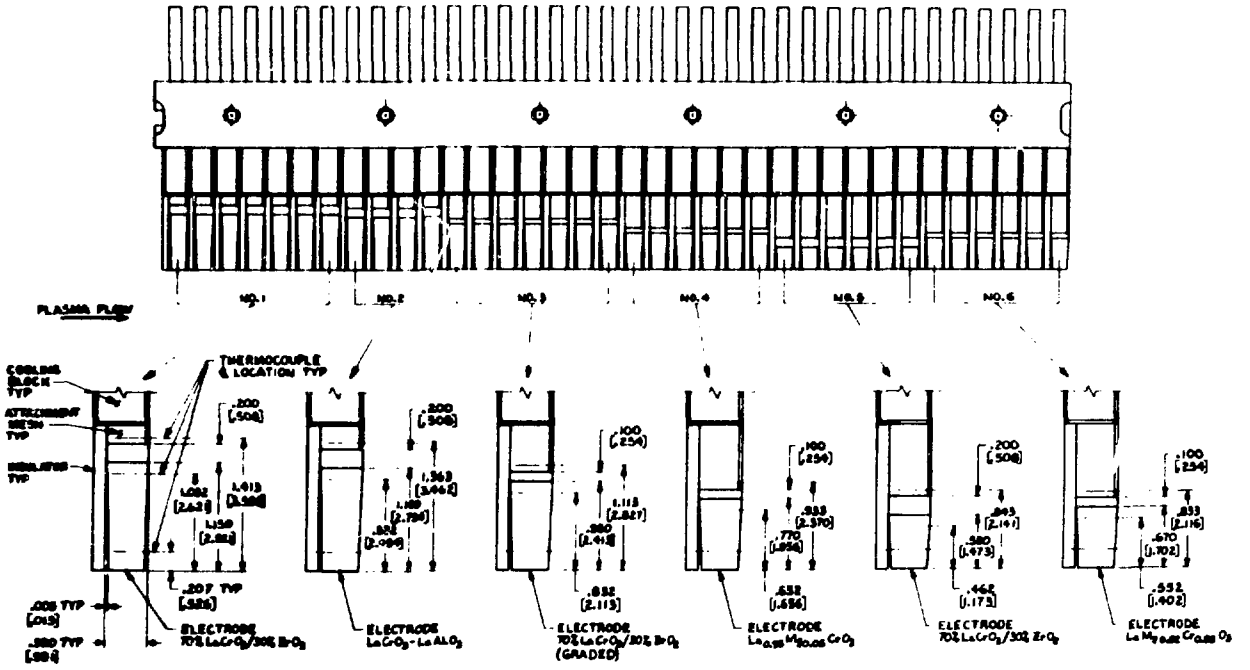

Figure 4. Electrode block diagram.

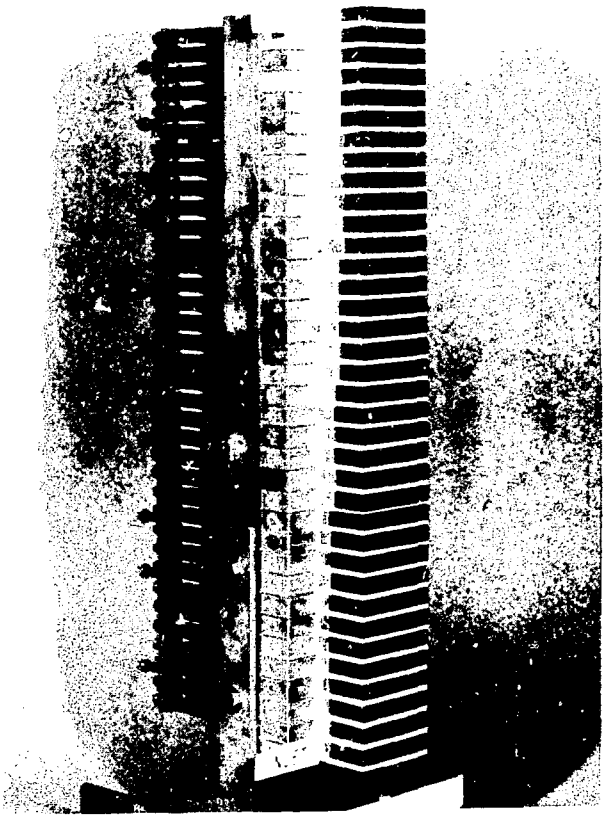

Figure 5. Electrode block prior to testing.

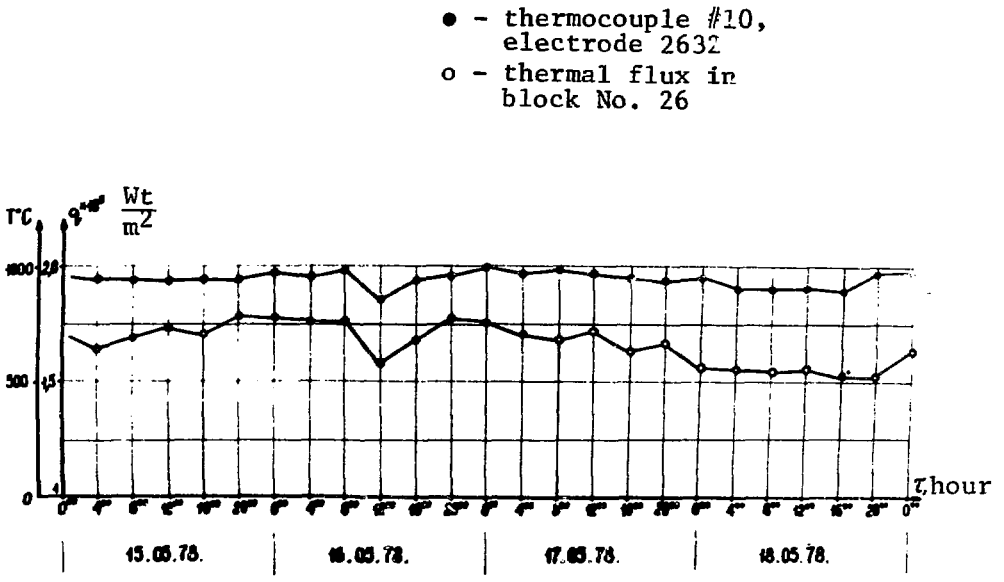

Figure 6. Change of thermal fluxes during experiment with the 6th group of electrodes (anode).

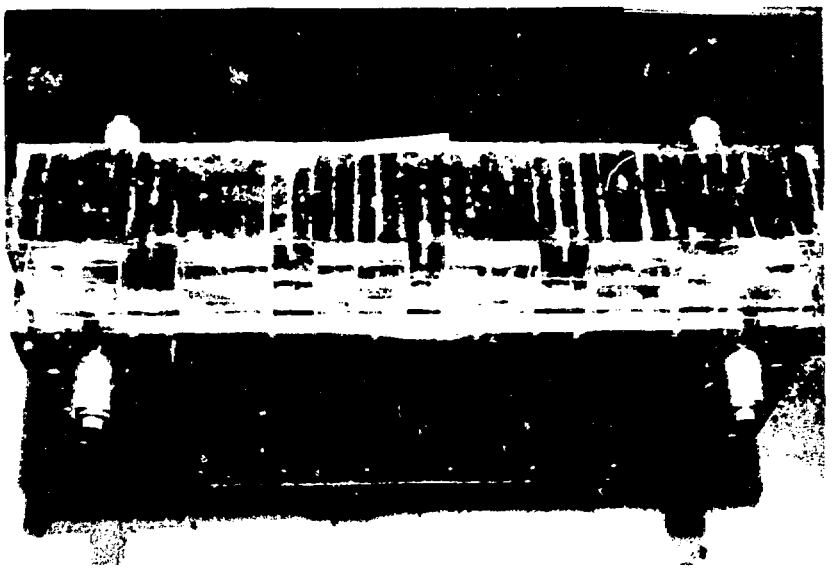

Figure 7. Electrode wall after test.

Figure 8. 2nd group of electrodes after test.

☆ U. S. GOVERNMENT PRINTING OFFICE : 1979 281-704, 1023